Waste Management 172 (2023) 171–181

Contents lists available at ScienceDirect

Waste Management

journal homepage: www.elsevier.com/locate/wasman

Research Paper

Pyrolysis of municipal solid waste: A kinetic study through multi-step reaction models

Alejandro Márquez [a,*], Elpida Patlaka [b], Stelios Sfakiotakis [b], Isabel Ortiz [a], José María Sánchez-Hervás [a]

[a] Unit for Sustainable Thermochemical Valorization, CIEMAT, Avenida Complutense, 40, 28040 Madrid, Spain
[b] Solid Fuels Beneficiation and Technology, Department of Mineral Resources Engineering, Technical University of Crete, University Campus 73100 Chania, Greece

ARTICLE INFO

Keywords:
Waste valorization
Thermogravimetric Analysis
Py-GC/MS
Isoconversional methods
Independent parallel reaction

ABSTRACT

The present study endeavors to establish a comprehensive kinetic analysis of Municipal Solid Waste residue pyrolysis. As the sample exhibits four distinct degradation stages, it has been carried out by adopting a multi-step process behavior. Different approaches have been compared, including five isoconversional methods (Kissinger-Akahira-Sunose, Ozawa-Flynn-Wall, Starink, Friedman and Advanced integral Vyazovkin), Mathematical Deconvolution Analysis, and Independent Parallel Reaction Model. The study focuses on the two active pyrolysis steps, the first one corresponds to the biomass components between 150 and 400 °C, with the decomposition peak between 300 and 350 °C, whereas the second corresponds to the plastic fraction with temperature ranging between 400 and 520 °C. The activation energy values obtained from the different kinetic methods for both steps are estimated at 240 and 250 kJ/mol, respectively. It was observed that the biomass components degradation obeys a third-order kinetic model, while the plastic fraction follows a first-order kinetic model. The analytical pyrolysis of the two main stages allows for the identification and semi-quantification of the compounds produced during municipal solid waste pyrolysis. Through analytical pyrolysis, it has been determined that up to 64 % of hydrocarbons are produced, of which 24 % correspond to aromatic compounds. Meanwhile, 20 % of oxygenated compounds were obtained, with ketones, furans, and acids being the most predominant families.

1. Introduction

Municipal solid waste (MSW) generation is estimated to increase by 70 % by the year 2050, reaching 3.4 billion tons (Khandelwal et al., 2019). Proper waste management is crucial for maintaining environmental sustainability and safeguarding public health, as inadequate handling of waste can result in air and water pollution, soil contamination, and the release of greenhouse gasses. (Khan et al., 2022). In terms of solid waste management technologies, open dumping and landfilling are commonly employed methods due to their low cost and simplicity, as they do not necessitate significant investments or advanced technologies. However, they have a large footprint, contributing to global warming if landfill gas is not captured for energy recovery, and could produce toxic and hazardous mature leachates if they are not adequately treated by advanced treatment trains (Said et al., 2023; Tejera et al., 2021). The scarcity of suitable landfill sites and the lack of assessments regarding the environmental impacts of landfilling, have resulted in the prohibition of landfilling combustible wastes, including wet organic waste, in many countries. According to the Sustainable Development Goal 11 (SDG 11), the proper management of municipal waste is critically significant in advancing sustainability and ensuring the preservation of natural resources for future generations (Alam et al., 2022). In this context, it is crucial to adopt advanced waste management practices to safeguard the environment, public health, ecosystems, and overall quality of life in the future. In recent decades, significant progress has been made in sustainable waste management, specifically in addressing the challenges of a circular economy. This involves the application of thermochemical technologies such as pyrolysis, gasification, or combustion, which promote waste reduction, reuse, recycling, and recovery. This shift from a linear to a circular economy aims to minimize landfilling and maximize resource utilization (Ingrao et al., 2018). Pyrolysis and gasification differ from incineration in the ability to recover the chemical value of the waste, rather than its energy. Among them, pyrolysis has gained attention in the last years due

* Corresponding author.
E-mail address: alejandro.marquez@ciemat.es (A. Márquez).

https://doi.org/10.1016/j.wasman.2023.10.031
Received 13 June 2023; Received in revised form 4 October 2023; Accepted 28 October 2023
Available online 1 November 2023

to its high efficiency and flexibility in generating a combination of solid, liquid and gaseous products, depending on the operational parameters (Laird et al., 2009). One of the main advantages of pyrolysis is its ability to treat a wide variety of waste types, including lignocellulosic biomass, plastics, hazardous waste such as medical waste, and, as is the focus of this study, MSW (Chew et al., 2021; Dharmaraj et al., 2021). In the context of waste management, MSW can be converted into fuel and safely disposable substances (such as char and metals) using the process of pyrolysis, therefore a pyrolysis reactor is an efficient waste-to-energy converter (Chen et al., 2015a). Kinetic analysis of MSW through pyrolysis process is critical for modelling the reactor design and provides a theoretical basis for scale-up. The behavior and kinetics research of each component present in the sample is essential to comprehending the pyrolysis process of complex MSW, being key to the conversion towards higher-value products (Garg et al., 2023; Mallick et al., 2023). The degradation of the sample, which is composed of multiple components and is therefore complex in nature, can be classified as a multi-step reaction. Despite the wide range of compositions within MSW and the varying thermal degradation behaviors of its components (Sørum et al., 2001), the application of mathematical models to predict the pyrolysis products, such as bio-oil yield, composition, and properties of the process is of a great importance, providing an understanding of the reaction kinetics.

Several studies related to kinetics of MSW pyrolysis can be found in the literature (Azam et al., 2020; Nzioka et al., 2019; Tang et al., 2018). However, these studies have focused solely on using rigid isoconversional methods, such as Kissinger-Akahira-Sunose (KAS); Ozawa-Flynn-Wall (OFW), and Starink without considering that it is a multi-step process. These isoconversional methods are highly useful when E_a remain nearly constant, suggesting that is a single-step process. However, for multicomponent samples, more suitable methods are required. Such as Mathematical Deconvolution Analysis (MDA) or Independent Parallel Reaction (IPR), which have not been previously explored or compared for the study of MSW pyrolysis. Some authors have studied the kinetics of MSW based on its most representative components such as cotton, cabbage, paper, and plastics, without actually conducting the study on a real MSW sample (Diaz Silvarrey & Phan, 2016; Dubdub & Al-Yaari, 2020; Zhang et al., 2015).

Therefore, the aim of this study is to present an insightful research in the kinetic modelling of municipal solid waste pyrolysis including a kinetic approach via thermogravimetric measurements and the determination of the kinetic parameters with the help of different modelling methods, some of them employing open-source software. The study consists of various modelling approaches, including isoconversional methods (KAS, OFW, Starink, and Advanced Integral Vyazovkin), MDA and IPR. The novelty of this study lies in the comparison of different multi-step kinetic methods on a real MSW sample. Additionally, for each decomposition stage, the composition of pyrolysis oil has been determined. The findings of this research will offer significant insights into the modeling of pyrolysis for MSW. This knowledge may help to create more efficient pyrolysis models, which could be crucial for improved municipal solid waste management and reduced environmental impact.

2. Materials and methods

2.1. Materials

The MSW residue was supplied by ECONWARD, a waste treatment company based in Madrid, Spain. Its technology is based on a thermal pressure hydrolysis system that uses steam to treat the organic fraction of MSW, the solid fraction obtained after the thermal pressure hydrolysis treatment was the sample studied in this study. The sample was prepared in the laboratory through homogenization and grinding. The sample was characterized using UNE-EN Standards, including proximate and ultimate analysis (EN 15402, EN 15403, EN 15407, EN 15408, EN 15410) moisture content (EN 15414–3), heating value (EN 15400), and ash composition (CEN/TR 15404), Table S1.

2.2. Chemical composition of the sample

The chemical composition of MSW residue was determined according to the National Renewable Energy Laboratory analytical procedures (Sluiter et al., 2008). Since the sample had been previously heat-treated, the extractive removal step was not carried out. The contents of glucans, xylans, arabinans, galactans, and mannans were determined by acid hydrolysis in two steps. First, the sample was subjected to an initial hydrolysis with sulfuric acid 72 % (w/w) (30 °C, 60 min) followed by a second hydrolysis with dilute sulfuric acid 4 % (v/v) (121 °C, 60 min), determining the sugars content of the hydrolysis liquors by HPLC. Sugars were determined through the procedure previously described (Moreno et al., 2021). The determination of the acid-insoluble residue was performed on the residue resulting from total hydrolysis with sulfuric acid. Starch content was determined in all samples by enzymatic method Total Starch Assay Kit (Megazyme, Ireland). The total nitrogen content of the acid-insoluble residue was determined by the conventional Kjeldahl method.

2.3. Thermogravimetric analysis

Thermal analysis system TGA 2 (Mettler Toledo Corporation, Switzerland) was used to measure mass and temperature variation versus temperature. TGA was performed at six different heating rates (5, 10, 15, 20, 25, and 40 °C/min) from 30 to 900 °C. The flow rate of the carrier gas (high-purity N_2) was set at a constant 50 mL/min. For each experiment, the sample weight was maintained at about 10 mg and it was placed in alumina crucibles avoiding contact with both sides of the oven. Previously to perform the analysis, temperature, weight, and platform calibrations were carried out.

2.4. Kinetic study

2.4.1. Isoconversional methods

Isoconversional methods are used to determine the activation energy and reaction rate constant of a chemical reaction by analyzing the reaction kinetics at different temperatures. These methods rely on multiple sets of experimental data obtained at different heating rates, a minimum of four. As a result, isoconversional methods can provide reliable initial kinetic parameters for modeling sections.

According to the one-step global model, the kinetic parameters of heterogeneous solid-state thermal decomposition can be described by the Arrhenius equation, Eq. (1). The Arrhenius equation is a fundamental equation in chemical kinetics that relates the reaction rate constant to temperature. The Arrhenius equation states that the reaction rate constant is exponentially dependent on temperature and can be expressed as:

$$\frac{d\alpha}{dT} = A exp\left(\frac{-E_a}{RT}\right) f(\alpha) \quad (1)$$

For non-isothermal TGA experiments at linear heating rate $\beta = dT/dt$, Eq. (1) can be written as Eq. (2):

$$\frac{d\alpha}{dT} = \frac{A}{\beta} exp\left(\frac{-E_a}{RT}\right) f(\alpha) \quad (2)$$

where, T is the absolute temperature (K), E_a is the activation energy (J/mol), A is the pre-exponential factor, R is the universal gas constant (J/mol^{-1}·K^{-1}) and β is the heating rate (K/s), and f(α) is the model function that depends on the reaction mechanism. Conversion rate (α) can be calculated according to Eq. (3), where m_0 is the initial mass (mg) and m_f is the final mass (mg).

$$\alpha = \frac{m_0 - m_\alpha}{m_0 - m_f} \tag{3}$$

Eq. (2) shows the dependence on two parameters (α and T), through the product of two functions, *k(T)* and *f(α)*. Based on this equation, several kinetics methods have been developed. This equation is based on the principle of a single-step reaction, and not on a multi-step process. For a single-step process, E_a should be nearly constant, so E_a does not fluctuate with α. The process is considered multi-step when variation in E_a reaches more than 20 % of the average (Vyazovkin et al., 2020). However, a multi-step process can be approximated as a single-step one at constant α and within a relatively small temperature range related to α (Vyazovkin et al., 2018). Some of the most popular isoconversional methods, such as Kissinger-Akahira-Sunose (KAS); Ozawa-Flynn-Wall (OFW), and Starink, are based on rigid integrations from a value of 0 to a given value of α, this approach significantly increases the variation of E_a in multi-step processes. In this article, three types of rigid integrative isoconversional methods are applied, KAS Eq. (4), OFW Eq. (5), and Starink Eq. (6). The derivation of these methods has been previously covered in literature (Flynn & Wall, 1966; Kissinger, 1957; Mishra & Mohanty, 2018; Starink, 1996; Takeo, 1965).

$$ln\left(\frac{\beta}{T^2}\right) = ln\frac{AR}{E_a G(\alpha)} - \frac{E_a}{RT} \tag{4}$$

$$ln\beta = ln\frac{0.0048AE_a}{RG(\alpha)} - 1,0516\frac{E_a}{RT} \tag{5}$$

$$ln\left(\frac{\beta}{T^{1.92}}\right) = C - 1.0008\frac{E_a}{RT} \tag{6}$$

This error does not occur by applying Friedman's differential method and is easily corrected in the Advanced integral Vyazovkin method, which employs numerical integration as part of the E_a assessment (Vyazovkin & Sbirrazzuoli, 2006). Friedman's method is not based on approximations and can be applied to any temperature rate while the Vyazovkin method is based on the integration over small segments of time. Friedman's method Eq. (7) and the Advanced integral Vyazovkin method Eq. (8) and Eq. (9) are presented (Friedman, 1964; Vyazovkin, 2000):

$$ln(\frac{d\alpha}{dt})_{\alpha,i} = ln[A_\alpha f(\alpha)\,] - \frac{E_\alpha}{RT_{\alpha,i}} \tag{7}$$

$$\Phi(E_\alpha) = \sum_{i=1}^{n}\sum_{j\neq 1}^{n}\frac{J[E_\alpha,\ T_i(t_\alpha)]}{J[E_\alpha,\ T_j(t_\alpha)]} \tag{8}$$

$$J[E_\alpha, T(t_\alpha)\,] = \int_{t_{\alpha-\Delta\alpha}}^{t_\alpha} exp\left[\frac{-E_\alpha}{RT(t)}\right]dt \tag{9}$$

Following the guidelines of ICTAC, and making the calculation procedures as transparent as possible, the open-source thermokinetic software THINKS is employed for calculating the Friedmann method as well as the Advanced integral Vyazovkin method. Nevertheless, these approaches yields favorable agreement for conversion rates within the range of 0.2–0.8. However, for values outside this range, alternative approaches should be considered for better fitting. Isoconversional methods are employed due to their capability to manage non-isothermal scenarios effectively. This enables the examination of changes in activation energy across various levels of conversion. This aspect is highly significant in deciphering the intricate and temperature-dependent reaction pathways found in MSW residue compositions.

2.4.2. Mathematical deconvolution analysis

In multi-step processes, such as those involving parallel, competitive or reversible reactions, or those complicated by diffusion, E_a varies with α. In such cases, α and T are no longer independent. To address this issue, an alternative approach is to deconvolute the constituent peaks from the TGA curves and analyze them separately (Muravyev et al., 2019). This method uses mathematical deconvolution, where peaks are separated empirically by summing the mathematically fitted component peaks, using a fitting function called F(t), where N is the total number of reactions, as shown in Eq. (10):

$$\frac{d\alpha}{dt} = \sum_{i=1}^{N} F_i(t) \tag{10}$$

This method is based on the assumption that each peak should represent an individual reaction step. Due to the asymmetric nature of rate peaks in single-step reactions, it is advisable to use mathematical functions with corresponding asymmetric peak shapes. The Frazer-Suzuki function is a well-established and effective function that has been successfully employed in mathematical deconvolution analysis Eq. (11) (Perejón et al., 2011):

$$F(t) = a_0 exp\left\{ - ln2\left[\frac{ln\left(1 + 2a_3\frac{x-a_1}{a_2}\right)}{a_3}\right]^2\right\} \tag{11}$$

In the Frazer-Suzuki equation, a_0, a_1, a_2, and a_3 represent the amplitude, position, half-width, and curve asymmetry, respectively. To perform the MDA, the software Origin Pro 8 SR4 was employed using the peak analysis method. The Frazer-Suzuki asymmetric equation was used for the simulated curves for all six heating rates (5, 10, 15, 20, 25, and 40 °C/min). MDA is used because they can untangle complicated reactions that happen together in mixed waste. This helps separate and identify distinct reaction steps, providing insight into how complex breakdown processes work.

2.4.3. Independent parallel reaction model

The Independent Parallel Reactions (IPR) model is a widely practiced kinetic model to analyze complex reaction systems. According to the IPR model, the decomposition of the materials can be described by three or more independent parallel first or n^{th} order reactions, each corresponding to the decomposition of the material constituents (Damartzis et al., 2011). The overall rate of conversion for N reactions and the thermal decomposition of the individual components can be expressed as Eq. (12) and Eq. (13):

$$\frac{dm}{dt} = -\sum_i c_i\frac{d\alpha_i}{dt}\, i = 1, 2, 3\cdots N \tag{12}$$

$$\frac{d_{ai}}{dt} = A_i exp(\frac{-E_i}{RT})(1 - a_i) \tag{13}$$

The finding of the optimal kinetic parameters (A, E_a) and the minimization of the error (deviation) between the experimental model and the theoretical model, was carried out after modeling in MATLAB code. The code has been developed in the Solid Fuel Refining and Technology Laboratory of the Technical University of Crete by Dr. Sfakiotakis for his doctoral. For the optimal parameters to be obtained (E_{ai}, A_i, c_i), which are minimized under constraints, the following objective function was used in Eq. (14):

$$O.F. = \sum_{k=1}^{N^{exp}}\sum_{i=1}^{N^p}\frac{\left(\frac{dm^{exp}}{dt}(t_i) - \frac{dm_{calc}}{dt}(t_i)\right)^2}{N^p\hat{A}\cdot(k)\hat{A}\cdot h(k)^2} \tag{14}$$

where N^p and N^{exp} represent the number of simultaneous fitting experiments and the number of experimental points ($i = 1,2,3\ldots N^p$) respectively, h(k) is the maximum rate of devolatilization and dm^{exp}/dt and dm^{calc}/dt the experimentally observed DTG curve and the calculated DTG curve. The denominator of Eq. (14) is related to the necessary scaling of the data due to the different number of experimental points

per experiment.

Finally, a deviation measurement between the experiment and the calculated curves at the optimal set of parameters was calculated for each experiment following Eq. (15), where z is the number of data points and N is the number of parameters employed in the model.

$$D(\%) = \frac{\sqrt{\frac{OF}{(z-N)}}}{max\left(-\frac{dm}{dt}\right)^{exp}} \hat{A}\cdot 100 \quad (15)$$

Since, IPR model allows for several concurrent reactions, its application is consistent with the actual nature of MSW residue pyrolysis. This method could present a more accurate illustration of the kinetics.

2.4.4. Model fitting

The determination of the kinetic parameters and the kinetic model was carried out using the procedure proposed by Pérez-Maqueda et al. (Pérez-Maqueda et al., 2006), which is based on a modification in the combined kinetic analysis using an empirical equation that fits every f (α) of the commonly used ideal kinetic models found in literature, as well as any deviations caused by differences in particle size distributions or variations in particle morphologies, Eq. (16). This approach offers the possibility of undertaking a combined kinetic analysis of experimental data obtained under any given conditions, without the need for prior assumptions regarding the kinetic model governing the reaction.

$$ln\left(\frac{\frac{d\alpha}{dt}}{(1-\alpha)^n \alpha^m}\right) = lncA - E/RT \quad (16)$$

From the values of n and m, the discrimination of the kinetic model is performed with the help of master plots. The parameters *n* and *m* was performed by the open-source thermokinetic software THINKS (Muravyev et al., 2019). This approach was also performed for each of the kinetic curve studied, isoconversional, MDA, and IPR. The reaction mechanism was studied employing the master plot method, where the experimental data is compared with standard curves to identify the mechanism function of the pyrolysis reaction (Criado et al., 1989). The most common ideal kinetic mechanism functions have been previously reported in numerous papers (Gotor et al., 2000; Liu et al., 2021; Luo et al., 2021; Noori et al., 2018).

2.5. Py-GC/MS analysis

Pyrolysis gas chromatography-mass spectrometry (Py-GC/MS) analysis was conducted to examine the products of pyrolysis in municipal solid waste (MSW). The Py-GC/MS system employed a CDS Analytical Pyroprobe (5200 HPR) coupled with an Agilent Technologies gas chromatography (7890A) and mass spectrometry (5975C) setup. Chemical species were separated through chromatographic techniques using an HP-5MS capillary column (30 m × 0.25 mm ID × 0.25 μm DF). The GC oven temperature was programmed to maintain 40 °C for 5 min, followed by a gradual increase to 280 °C at a rate of 5 °C/min. The temperature was then held constant at 280 °C for 15 min. The injection port was maintained at 300 °C, and a carrier gas flow rate of 1 mL/min with a split ratio of 1:75 was used. The 5975C mass spectrometer operated in SCAN mode, with a mass range of *m/z* 10–500 amu. The electron energy was set to 70 eV, and the transfer line and ion source were maintained at 250 °C. High-purity helium was utilized as both the carrier and purge gas in the Py-GC/MS system. The chromatographic data were processed using MDS ChemStation (E.02.02.1431) software, and mass spectra laboratory databases (NIST08 v2.0) were employed for identification and semi-quantification.

Py-GC/MS tests of MSW were carried out using a heating ramp of 40 °C/min from 30 °C to 900 °C. The pyroprobe 5200 HPR interface was set at 300 °C to avoid condensation in the equipment, and both the transfer line and valve oven were maintained at 300 °C. The volatile compounds released during pyrolysis were captured using a tenax trap. Once the pyrolysis process was completed, the retained compounds were desorbed by increasing the temperature of the trap to 300 °C. At that point, the compounds were analyzed using GC/MS. Three different experiments were conducted. The first involves pyrolysis of the MSW at 40 °C/min from 30 °C to 900 °C, simulating TGA conditions. The second experiment was pyrolysis at 40 °C/min from 30 to 400 °C to identify and semi-quantify the compounds produced during the second stage of the MSW degradation. Afterward, the same sample was subsequently pyrolyzed at a heating rate of 40 °C/min in the range of 400–600 °C to determine the compounds produced during the third degradation stage.

3. Results and discussion

3.1. Chemical composition analysis of the sample

Table 1 displays the results of the sample's chemical composition analysis as well as the ash composition. Although MSW is known for its varied (or heterogeneous composition), which can vary not only between sites but also over time. It is worth noting the sample's high ash content of 27 %. This could be explained due to a previous subjected thermal pressure hydrolysis process of the sample, yielding a greater percentage of ashes. The major oxides contained in the ashes are SiO_2 and CaO, accounting for 29 % and 25 % of the total ash, respectively. Despite being thermally hydrolyzed, the sample contains a significant quantity of structural carbohydrates, with 20.5 % of cellulose and 7.6 % of hemicellulose, and other components such as proteins with 11.4 %. Finally, the insoluble acid residue would correspond to the percentage of lignin in the case of a pure biomass sample (Negro et al., 2017). However, since it is an MSW residue, the acid-insoluble residue value likely corresponds to the presence of plastics, or a mixture of lignin and plastics. The remain portion until reaching 100 % are extractable and soluble compounds in organic solvents and acids that have not been identified.

3.2. Thermogravimetric analysis of the sample

Fig. 1 presents the TGA and DTG curves for the sample at six different heating rates (5, 10, 15, 20, 25, and 40 °C/min). Based on the data, the sample decomposition can be divided into four stages. The first stage corresponds to moisture and volatile loss (~4 % mass loss) between 80 and 150 °C, which is slightly lower than the obtained value. During the second stage, between 150 and 400 °C, most of the sample degradation occurs (greater than 40 % mass loss) with the decomposition peak between 300 and 350 °C, this stage represents an "active pyrolysis zone".

Table 1
Chemical composition of MSW residue.

Component	MSW
Cellulose	**20.5 ± 1.2**
Hemicellulose	**7.6 ± 0.5**
Xylan	3.4 ± 0.1
Galactan + Arabinan + Mannan	4.2 ± 0.4
Acid-insoluble residue	**26.6 ± 0.1**
Proteins	**11.4 ± 0.1**
Starch	**3.9 ± 0.1**
Ashes	**27.0 ± 1.2**
SiO_2[a]	29
CaO[a]	25
Al_2O_3[a]	5.6
Na_2O[a]	4.6
SO_3[a]	4.6
K_2O[a]	4.5
Unidentified compounds	**3.0 ± 3.2**
Total	**100 ± 4.3**

Data in percentage of total on a dry matter basis.
[a] Percentage of ash content.

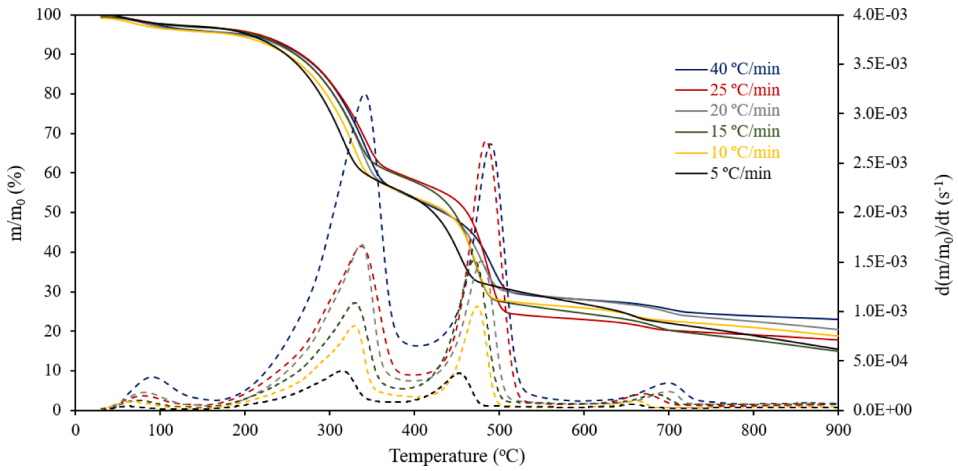

Fig. 1. TG (solid lines) and DTG (dotted lines) curves for MSW at six different heating rates.

The decomposition of the typical components of biomass, cellulose, hemicellulose, and proteins occurs at this stage, matching the results found in the chemical composition analysis. Although several components undergo decomposition during this stage, no shoulders are observed in the DTG curve, and only a peak is visible around 320 °C. The third stage occurred between 400 and 520 °C (~27 % mass loss) and is proceeded by the reaction of the plastic fraction. Since the mass loss at this stage corresponds to the percentage of insoluble acid residue (26.6 %), it is possible to conclude that the insoluble acid residue corresponds fully to the plastics fraction thus the sample contains no lignin. The fourth stage refers to char degradation (a 10 % mass loss), and is considered a "passive pyrolysis zone", it occurs throughout a wide temperature range of 550–900 °C. During this phase, the remaining sample that was carbonized in the second and third stages undergoes partial devolatilization. Finally, at 900 °C, a final mass of char of 18.4 % ± 3.1 % was obtained, a significantly higher value if compared to other biomasses with lower ash content.

3.3. Kinetic study

3.3.1. Isoconversional methods

According to ICTAC recommendations (Vyazovkin et al., 2020) for multi-step kinetics analysis, the first approach is to determine the variation of E_a with α. In the case that the variation is greater than 20 %, it can be determined that it is a multi-step process. For this purpose, integral methods such as KAS, OFW, Starink, and the Advanced Integral Vyazovkin method, as well as derivative methods such as Friedman's method, have been employed. Fig. 2 displays the values obtained of E_a as a function of the conversion (α) for the previously mentioned methods.

MSW activation energy stays constant during the first stage of biomass decomposition when a is between 0.2 and 0.4. During this stage, all of the isoconversional methods studied showed relatively consistent E_a values, around 205 kJ/mol. Then, from 0.5 to 0.6 the activation energy decreases to 20 kJ/mol average, the present phase marks the transition from the biomass degradation stage to the plastic fraction decomposition, occurring within the temperature interval of 350–430 °C. Notably, a decline in the rate of decomposition is observed during this phase, as can be seen in Fig. 1. Isoconversional methods are based on the assumption that the activation energy is temperature independent. However, in some cases, the activation energy may decrease as the temperature increases, this phenomenon is known as the compensation effect. The compensation effect can be observed during exothermic reactions that release a large amount of heat during their progress. As the temperature increases, the heat release increases, reducing the activation energy required for the reaction to continue (Vyazovkin, 2015). From the conversion of 0.7 onwards, the activation energy increases, exceeding 250 kJ/mol. Within this conversion range, the decomposition of the plastic fraction in the sample occurs. It is at this stage when the results obtained by different isoconversional methods differ considerably, except for the most popular ones among the literature, KAS, OFW, and Starink. This reveals trivial differences in the values of E_a obtained by these methods, and hence the need to use more accurate methods such as the Friedman differential method or the Advanced Integral Vyazovkin method. The variation observed in the activation energy, as presented in Fig. 2, provides evidence that the reaction mechanism of MSW pyrolysis could involve complex, competing, and parallel reactions.

Each step in the multi-step kinetic model should follow a specific reaction model. Various reaction models produce rate peaks with varying shapes. If the peak is visible, the reaction model can be determined by fitting the experimental data, just as it is for single-step reactions (Vyazovkin et al., 2020). As the experimental data displays two distinct and noticeable peaks corresponding to the degradation stages 2 and 3, isoconversional analysis can be performed separately for each stage, treating them as single-step reactions and taking into account the conversion for each stage. Fig. 2 also displays the activation energy values for the second degradation stage between 150 and 400 °C and the third degradation stage between 400 and 520 °C. The obtained results exhibited a high level of accuracy, as evidenced by the excellent statistical correlation with the R^2 factor exceeding 0.9 over the conversion range of 0.2 to 0.8.

The second stage of degradation corresponds to the decomposition of components derived from biomass materials (cellulose, hemicellulose, and proteins). The mean activation energy values estimated are 243 kJ/mol (KAS), 240 kJ/mol (OFW), 243 kJ/mol (Starink), 244 kJ/mol (Advanced Integral Vyazovkin), and 258 kJ/mol (Friedman) for the second degradation stage. Overall, the results indicate that there are only minor variations among the methods used. Notable, the main discrepancies are observed between the derivative Friedmańs method and the other approaches, whereas the integral methods exhibit a high level of correlation.

The third stage of degradation corresponds to the pyrolysis of the plastic fraction. The average activation energy values obtained are 248 kJ/mol (KAS), 247 kJ/mol (OFW), 248 kJ/mol (Starink), 240 kJ/mol (Advanced Integral Vyazovkin), and 252 kJ/mol (Friedman). Similar to the results from the second stage of degradation, the findings calculated using integral methods (KAS, OFW, and Starink) exhibit trivial differences, while more precise methods show greater variation.

The E_a obtained value for the degradation of the biomass compounds falls within the range previously reported by Arenas et al. for waste food simple (Arenas et al., 2019) or Fang et al. for MSW and paper sludge (Fang et al., 2018), where values ranging from 180 to 250 kJ/mol were

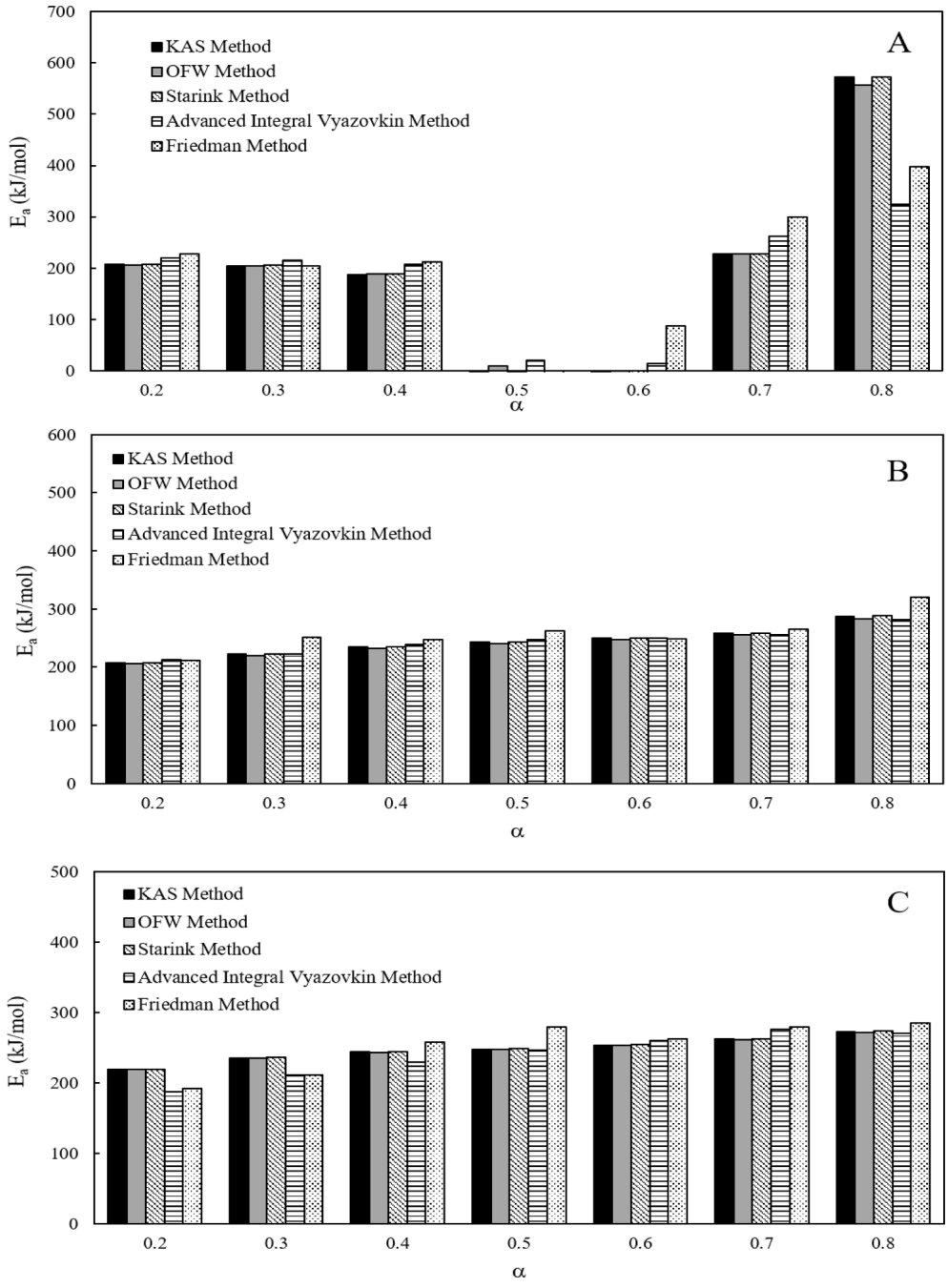

Fig. 2. Activation energy (Ea) dependencies on the conversion fraction (α) from 0,2 to 0,8 for MSW employing different isoconversional methods, (A) for the whole process (30–900 °C), (B) for the second stage (150–400 °C) and (C) for the third stage (400–520 °C).

reported. In the latter case, the authors studied the kinetic behavior using the Distributed Activation Energy Model (DAEM), considering four parallel and irreversible reactions (first-order). While this approach provides reliable values for the activation energy, the challenge lies in the subsequent calculation of the pre-exponential factor, as all reactions share the same value (Chen et al., 2015b). On the other hand, the activation energy obtained during the degradation of plastics also resembles values obtained in kinetic studies of plastics individually and in co-pyrolysis. In this case, the values obtained for polylactic acid (PLA), polystyrene (PS), polyethylene terephthalate (PET), and polypropylene (PP) are between values of 235–279 kJ/mol (Navarro et al., 2018).

While isoconversional techniques eliminate many of the disputes associated with model fitting and single-heating-rate approaches, they still possess shortcomings. When various methods are employed on identical non-isothermal data, disparate outcomes are generated (Mianowski et al., 2021). The assumptions utilized to develop integral methods stand as a significant point of contention and a noteworthy origin of error (Dhyani & Bhaskar, 2018). Additionally, a debate exists regarding the fundamental nature of isoconversional methods, as they lack the ability to anticipate reaction mechanisms or preexponential factors.

3.3.2. *Mathematical deconvolution analysis*

By using the Frasez-Suzuki deconvolution, the pyrolysis of MSW can be divided into two single reactions. Table 2 lists the MDA results for MSW at heating rates of 5, 10, 15, 20, 25, and 40 °C/min. The MDA using Frasez-Suzuki fits the experiments with values of R^2 over 0.9. The average values of the area under the curve for each of the reactions

Table 2
Fitting results of Mathematical deconvolution analysis using Frazer-Suzuki function.

	Parameter	40 °C/min	25 °C/min	20 °C/min	15 °C/min	10 °C/min	5 °C/min
2 Peaks	R^2 adjust	0.956	0.973	0.943	0.958	0.940	0.948
	RSS	3.87E-05	1.92E-05	2.55E-05	1.54E-05	1.58E-05	2.50E-06
	$\chi 2$	2.42E-08	8.05E-09	8.79E-09	4.09E-09	2.86E-09	4.65E-10
	Area 1 (%)	66.67	55.20	65.84	55.33	61.24	64.83
	Area 2 (%)	33.33	44.80	34.16	44.67	38.76	35.16

obtained in the MDA correspond to the results of the chemical composition analysis and TGA values, being 61.5 % for the first reaction and 38.5 % for the plastic decomposition reaction. Fig. S1 presents the curves obtained through MDA of MSW pyrolysis at different heating rates.

3.3.3. Independent parallel reaction

As previously mentioned, the code was contacted in a MATLAB environment. The algorithm (Fig. S2) initially receives experimental values extracted from the laboratory experiments, including the mass and rate of mass loss of the biomass sample for a specific temperature. Subsequently, the noise is subtracted, and the temperature range within which specific pseudo-components undergo degradation is determined. This process also determines the number of components that participate in the reaction and the order of the reaction. The linearization process is subsequently repeated in each experimental zone, utilizing regression techniques to calculate the values of Ea_i and A_i, assuming a first-order reaction. During the execution of the algorithm, restrictions concerning the values of E_a, A, and c were imposed. Specifically, the activation energy was limited to 350 kJ/mol, while the pre-exponential factor was restricted to values ranging between 10^8 and 10^{21} min^{-1}. The limitations were set considering the best deviation for the model and the bibliographic data (Martínez-Narro et al., 2023; Sørum et al., 2001). Values of *c* exceeding unity were not permitted. Next, the algorithm calculates initial sample values for each component through vector quadrature (quadv) and non-linear functions optimization (fmincon) before performing the first minimization procedure with the calculation of Eopt1, Aopt1, and copt1. Following this, the algorithm uses these initial values to perform a second and third minimization process, ultimately providing the results of the sample. If the values and deviations of theoretical and modelling values are unacceptable, the algorithm continues iterations; otherwise, it terminates.

The IPR model presents an advantage over the mathematical deconvolution method, as it allows for the addition of reactions independently of the number of peaks identified by thermogravimetry. Chemical composition analysis determined the main components present in the MSW sample (hemicellulose, cellulose, proteins, and plastic fraction). Therefore, one reaction has been established for each pseudo-component. The first reaction accounts for the hemicellulose component, whereas the second reaction accounts for the cellulose component. The third reaction signifies the proteins present in the samples. The fourth and final reaction pertains to the 3rd degradation stage and encapsulates the plastic fraction within the sample. The results of the IPR method parameters are shown in Table 3. Regarding the hemicellulose reaction, it is noteworthy that according to simultaneous fitting, the activation energy (E_a) is equal to 68.1 kJ/mol. As for the cellulose component, the activation energy has the respective value of 116 kJ/mol, while for the protein component, the activation energy is equal to 168 kJ/mol. The values reported in this study agree with those reported by other authors in literature from other biomass-related subjects. For instance, Nisar et al. obtained activation energy values of 121.2 kJ/mol and 71.1 kJ/mol for cellulose and hemicellulose, respectively (Nisar et al., 2021). On the other hand, regarding protein, Simão et al. reported values around 146–149 kJ/mol. Values slightly lower than those reported in this study may be attributed mainly to the disparity in the method used for their calculation and the distinct nature of the studied biomass (Simão et al., 2018).

Table 3
IPR kinetic parameters (Ea, A and c) under different heating rates.

	Parameter	Simultaneous Fitting
Reaction 1	E_1 (kJ/mol)	68.1
	$Ln(A_1)$ (s^{-1})	13.8
	C_1 (%)	8.5
Reaction 2	E_2 (kJ/mol)	116.2
	$Ln(A_2)$ (s^{-1})	21.9
	C_2 (%)	12.7
Reaction 3	E_3 (kJ/mol)	168.4
	$Ln(A_3)$(s^{-1})	31.0
	C_3 (%)	5.1
Reaction 4	E_4 (kJ/mol)	210.6
	$Ln(A_4)$ (s^{-1})	30.2
	C_4 (%)	24.5

Notably, the plastic component displays the highest activation energy with the value of 211 kJ/mol. The activation energy values of the plastic fraction are similar to those obtained using isoconversional methods (200–250 kJ/mol), indicating that the results are reliable. However, comparing the IPR method with isoconversional methods for the second stage of degradation, which involves the decomposition of hemicellulose, cellulose, and proteins, is challenging because the isoconversional method groups these reactions together, while the IPR model considers them separately. The curves obtained can be found Fig. S3.

3.3.4. Determination of the reaction mechanism

By employing MDA, two sets of curves were obtained for each heating rate corresponding to the degradation stage of the biomass components and the plastic fraction. On the other hand, using the IPR method, four curves were obtained corresponding to the degradation of each of the pseudo-components present in the sample (hemicellulose, cellulose, proteins, and plastic). Therefore, experimental reaction (1) with MDA comprises reactions (1), 2, and 3 of IPR, while experimental reaction (2) with MDA is comparable to reaction (4) of IPR.

The experimental and simulated curves data were analyzed using the open-source thermokinetic software THINKS for determining the kinetic parameters without any prior assumptions (Eq. (16)). Table 4 presents the results of the kinetic parameters of the experimental and simulated curves (MDA and IPR).

The result from Table 4 shows that the activation energy value for the 1st reaction, determined from both experimental and MDA curves, remains stable at approximately 240 kJ/mol. This value falls within the range obtained when applying isoconversional methods (Fig. 2). Similarly, the E_a values obtained for the plastic degradation stage are consistent with those reported in the literature and those calculated using isoconversional approximation, with values hovering around 200–250 kJ/mol.

On the other hand, the results derived from IPR curves reveal the challenges encountered in accurately determining and optimizing kinetic parameters with this method when dealing with pseudo-components that are presented in the same degradation stage, such as 1st Reaction, 2nd Reaction, and 3rd Reaction, which correspond to the degradation of hemicellulose, cellulose and proteins. This leads to unreliable data, specially obtaining much higher E_a values than those

Table 4
Activation energy, pre-exponential factors, n and m parameters obtained from Eq. (16) for experimental, MDA and IPR curves of municipal solid waste pyrolysis.

Parameter	Experimental		MDA		IPR			
	1st Reaction	2nd Reaction	1st Reaction	2nd Reaction	1st Reaction	2nd Reaction	3rd Reaction	4th Reaction
n	0.44 ± 0.05	0.87 ± 0.06	2.66 ± 0.10	1.81 ± 0.15	5.31 ± 0.08	1.56 ± 0.08	1.51 ± 0.05	1.96 ± 0.14
m	−3.12 ± 0.05	−0.01 ± 0.06	−1.4 ± 0.05	0.25 ± 0.15	−1.21 ± 0.08	−1.32 ± 0.08	−1.35 ± 0.05	0.23 ± 0.14
E_a (kJ/mol)	238.9 ± 2.2	253.4 ± 3.1	238.1 ± 2.2	258.7 ± 6.4	247.3 ± 3.6	313.7 ± 6.8	188.1 ± 2.3	218.7 ± 5.9
Ln(A) (s^{-1})	41.3 ± 0.4	36.5 ± 0.5	43.4 ± 0.9	38.1 ± 1.1	51.3 ± 0.8	58.0 ± 1.4	30.3 ± 0.4	31.1 ± 1.0
R^2	0.9651	0.9313	0.9552	0.9560	0.9767	0.9701	0.9818	0.9590

reported in the literature and those obtained through the Matlab code, as reflected in Table 3 during biomass degradation.

The reaction model was established by comparing the reduced f(α)/f(0.5) with the ideal kinetic reactions types, as shown in Fig. 3. This comparison was carried out after determining *m* and *n* parameters for each reaction and curve (experimental, MDA and IPR). According to the findings, the biomass components degradation of the experimental and MDA curves follows a third-order reaction (F3), while the plastic pyrolysis aligns with a first-order reaction (F1). Similarly, for the curves obtained through the IPR Matlab code, the decomposition of biomass pseudo-components (hemicellulose, cellulose, and proteins) are consistent with a third-order reaction (F3), while the plastic breakdown approximates to a first-order reaction (F1).

The understanding of activation energy and kinetic model gained from this kinetic study holds significant implications for the scale-up and industrial utilization of the MSW residue valorization process, enabling informed decisions on temperature optimization and reactor design to enhance efficiency and viability at larger production scales.

3.4. Determination of compounds produced during MSW pyrolysis stages

In this study, analytical pyrolysis was performed to identify and semi-quantify the composition of the volatile fraction obtained for different tests, after identifying the two main degradation stages of the MSW sample. The sample was subjected to complete pyrolysis up to 900 °C at a heating rate of 40 °C/min, followed by two additional tests to determine the compounds produced during the second (150–400 °C) and third degradation stages (400–600 °C), respectively. The results, presented in Table 5, clearly indicate a substantial variance of product distribution in each pyrolysis stage, which were categorized according to their chemical structure for comparison purposes. The volatile products generated within the temperature range of 150–400 °C are associated with the pyrolysis of biomass fraction components; hence, E_a obtained in the kinetic study for that temperature range can be attributed to biomass pyrolysis. Similarly, the compounds produced during pyrolysis from 400 to 600 °C can be linked to the decomposition of the plastic fraction, and therefore, the previously determined E_a can be referred to as plastic pyrolysis.

The degradation produced from 150 to 400 °C was attributed to the

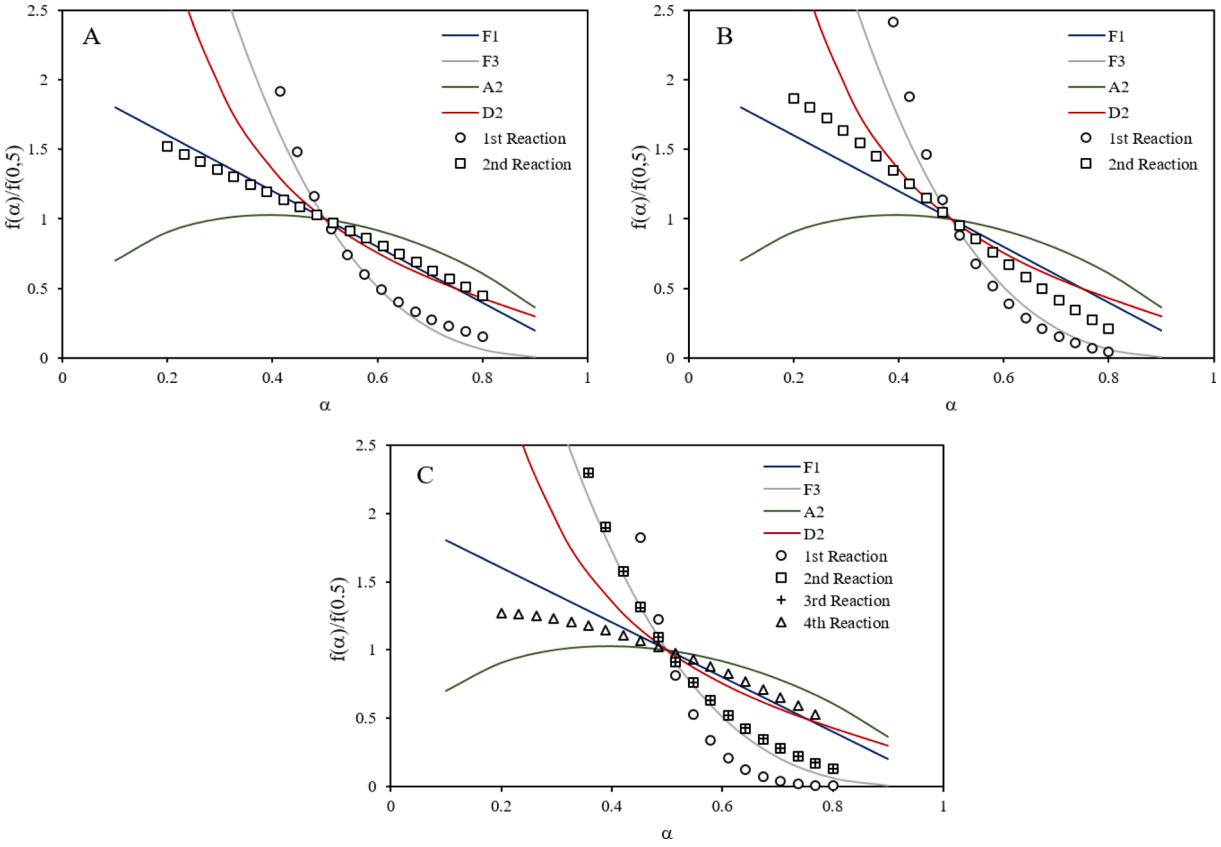

Fig. 3. Comparison of the f(α) of the first and second reaction obtained experimental (a), MDA curves (b) and IPR model (c) with the some of the ideal kinetic models.

Table 5
Volatile composition produced during MSW pyrolysis at 40 °C/min, including pyrolysis from 30 to 900 °C, first reaction pyrolysis from 30 to 400 °C, and second reaction pyrolysis from 400 to 600 °C.

	MSW 30-900 °C	MSW 150-400 °C	MSW 400-600 °C
Hydrocarbons	**64.28**	**2.09**	**64.32**
Aromatic	22.67	2.09	23.98
Alifatics	41.61	0.00	40.34
Alkenes	30.40	0.00	29.10
Alkanes	11.21	0.00	11.24
Oxygenated	**19.49**	**64.80**	**13.41**
Ketones	6.98	24.89	4.63
Acids	2.94	9.46	0.00
Phenols	3.88	5.67	6.02
Furans	3.29	16.38	0.50
Alcohols	1.39	2.38	2.27
Aldehydes	0.50	3.12	0.00
Pyrans	0.00	0.73	0.00
Sugars	0.50	2.16	0.00
Nitrogenous	**1.11**	**1.91**	**2.60**
Pyrroles	1.11	1.91	1.39
Lactams	0.00	0.00	1.21
Unknown	**15.12**	**31.20**	**19.67**
Total	**100**	**100**	**100**

Data in weight-normalized TIC areas (%).

decomposition of biomass constituents (cellulose, hemicellulose, and proteins), with oxygenated compounds reaching their maximum, accounting for 64.5 % of the total. The pyrolysis of cellulose and hemicellulose primarily produced a significant amount of ketones, acids, and aldehydes, accounting for 24.9 %, 9.56 %, and 3.12 %, respectively (Lv & Wu, 2012; Wu et al., 2013). Additionally, a bio-oil with a high content of O-heterocyclic compounds, such as furan derivatives, produced during the decomposition of glucose was obtained, accounting for 16.4 % (Ma et al., 2019). In general, hemi-cellulose displayed several pyrolysis routes. These included dehydratation and depolymerization, removing water to produce furan and pyran ring variations, and breaking furanose and pyranose rings to form less complex oxygenated compounds, The activation energy for these processes has been determined within this study to be 71.1 kJ/mol. In addition, the main cellulose pathways involves also the depolymerization into anhydrosugars and then the ring-brakage to produce lighter oxygenated compounds (Cai et al., 2019). The activation energy for this cellulose degradation mechanism has been established at 121.2 kJ/mol. Protein breakdown resulted in the production of nitrogen compounds, with pyrroles (1.91 %) being the most relevant among them, along with oxygenated compounds such as phenols (5.67 %) (Shahbeig & Nosrati, 2020).

At 400 °C, the pyrolysis of the plastic fraction took place, leading to a significant decrease in the proportion of oxygenated compounds to 13.1 %, while hydrocarbons increased up to 64.3 %. According to the literature, the pyrolysis of plastics such as PE, PS, or PP generates a significant quantity of aromatic hydrocarbons, particularly those with a single-ring structure (Sophonrat et al., 2017). In the case of MSW pyrolysis, styrene (7.52 %), and toluene (4.43 %) were identified as the most prominent aromatic hydrocarbons, accounting for 24 % of the total. This value is slightly higher than that obtained in MSW pyrolysis carried out between 30 and 900 °C. Moreover, in pyrolysis at 400–600 °C, aliphatic compounds accounted for more than 40 % of the bio-oil composition, with alkenes being the most abundant (72 % of aliphatic compounds). Jung et al. (Jung et al., 2010) reported that oil derived from PP and HDPE pyrolysis mainly comprises aliphatic and monoaromatic hydrocarbons, with the majority of compounds being C_6-C_{13} alkenes, benzene, toluene, ethylbenzene, and styrene. These compounds are those obtained mainly during the pyrolysis of MSW from 400 °C to 600 °C. The reported activation energy values for PP, PS, and HDPE in the literature are 220–259 kJ/mol, 153–265 kJ/mol, and 170–200 kJ/mol, respectively (Ali et al., 2020; Encinar & González, 2008). The activation energy values for the plastic fraction degradation in this study fall within the reported range in the literature. This factor, along with the major compounds produced in this stage, allows us to estimate that the main plastics present in the MSW residue sample are PP, HDPE, and PS. The bio-oil obtained from the mixed plastic pyrolysis exhibits a composition that is comparable in quality to that of the bio-oil produced from individual plastic pyrolysis (Lou et al., 2022; Pal et al., 2023). The properties of bio-oil, including its high aliphatic and monoaromatic hydrocarbon composition, sustainably sourced, reduced carbon footprint, and compatibility with existing infrastructure, make it a promising option for integration into petrochemical refineries, offering both environmental and economic benefits, while also aiding in compliance with regulations related to renewable content and emissions reduction (Anuar Sharuddin et al., 2016).

Even though pyrolysis is considered a sustainable waste-to-energy technology, presents challenges when applied to biomass and specially MSW residues. These challenges include low energy density and the creation of undesired by-products like tars, nitrogen compounds, and oxygenated substances (phenols, ketones, aldehydes, and acids) as reported in Table 5 (Gao et al., 2022). Despite these challenges, these compounds hold promise for diverse applications. Both aromatic and aliphatic hydrocarbons have potential uses. The petrochemical industry uses aromatics (benzene, toluene, and xylene) to make chemicals, plastics, textiles, and medications. Alkanes and alkenes, such as methane for clean burning energy and alkenes for polymers, are essential fuel sources (Bustillo-Lecompte et al., 2018). The oxygenated compounds produced by the pyrolysis of biomass components, mainly ketones, acids, and furans, reduce the quality of the produced bio-oil. Catalytic pyrolysis, with catalysts such as zeolites and bimetallics, offers an improvement in the process by reducing the presence of oxygenated compounds and increasing the production of higher value-added compounds (Li et al., 2020; Sipra et al., 2018).

In order to analyze the gases generated during pyrolysis, it is necessary to conduct laboratory-scale experiments and accurately determine the yield of each fraction. It is vital to consider the potential formation of chlorinated compounds that might arise from PVC fractions, which could lead into corrosion (Chen et al., 2014). Additionally, the presence of sulfur compounds (Hasan et al., 2021), unidentifiable through the Py-GC/MS technique used, should also be taken into account.

4. Conclusions

Isoconversional methods and MDA rely on the identification of two reactions, while the IPR model uses four independent reactions based on chemical composition. The activation energy values obtained by isoconversional methods and MDA for the pyrolysis of biomass components and the plastics fraction indicate values around 240 kJ/mol and 250 kJ/mol, respectively. In addition, biomass components degradation obeys a F3 reaction, while plastic pyrolysis follows a F1 reaction. The analytical pyrolysis of each of the two main stages allows for the identification and semi-quantification of the compounds produced during the degradation of MSW residue. The significance of this study lies in obtaining a deeper understanding of the thermal transformation process of real MSW. The derived activation energy values can aid in reactor design, temperature optimization, and predicting reaction rates, thereby contributing to the efficient transformation of MSW into more valuable products. Moreover, the identified kinetic behaviors of biomass components and plastic degradation provide insights for developing time–temperature profiles that enhance product yields and selectivity, ultimately improving overall conversion efficiency.

Declaration of competing interest

The authors declare that they have no known competing financial interests or personal relationships that could have appeared to influence the work reported in this paper.

Data availability

No data was used for the research described in the article.

Acknowledgment

The authors gratefully acknowledge financial support from the Community of Madrid for the project S2018/EMT-4459 (RETO-PRO-SOST2-CM) and Program DESCARTES, "Development of water and biogas purification materials from waste pyrolysis" financed by Spanish Ministry of Science and Innovation, TED2021-130147B-C22.

Appendix A. Supplementary material

Supplementary data to this article can be found online at https://doi.org/10.1016/j.wasman.2023.10.031.

References

Alam, S., Rahman, K.S., Rokonuzzaman, M., Salam, P.A., Miah, M.S., Das, N., Chowdhury, S., Channumsin, S., Sreesawet, S., Channumsin, M., 2022. Selection of Waste to Energy Technologies for Municipal Solid Waste Management—Towards Achieving Sustainable Development Goals. Sustainability 14 (19), 11913.

Ali, G., Nisar, J., Iqbal, M., Shah, A., Abbas, M., Shah, M.R., Rashid, U., Bhatti, I.A., Khan, R.A., Shah, F., 2020. Thermo-catalytic decomposition of polystyrene waste: Comparative analysis using different kinetic models. Waste Manag. Res. 38 (2), 202–212. https://doi.org/10.1177/0734242x19865339.

Anuar Sharuddin, S.D., Abnisa, F., Wan Daud, W.M.A., Aroua, M.K., 2016. A review on pyrolysis of plastic wastes. Energ. Conver. Manage. 115, 308–326. https://doi.org/10.1016/j.enconman.2016.02.037.

Arenas, C.N., Navarro, M.V., Martínez, J.D., 2019. Pyrolysis kinetics of biomass wastes using isoconversional methods and the distributed activation energy model. Bioresour. Technol. 288, 121485 https://doi.org/10.1016/j.biortech.2019.121485.

Azam, M., Ashraf, A., Jahromy, S.S., Raza, W., Khalid, H., Raza, N., Winter, F., 2020. Isoconversional nonisothermal kinetic analysis of municipal solid waste, refuse-derived fuel, and coal. Energy Sci. Eng. 8 (10), 3728–3739. https://doi.org/10.1002/ese3.778.

Bustillo-Lecompte, C.F., Kakar, D., Mehrvar, M., 2018. Photochemical treatment of benzene, toluene, ethylbenzene, and xylenes (BTEX) in aqueous solutions using advanced oxidation processes: Towards a cleaner production in the petroleum refining and petrochemical industries. J. Clean. Prod. 186, 609–617. https://doi.org/10.1016/j.jclepro.2018.03.135.

Cai, H., Liu, J., Xie, W., Kuo, J., Buyukada, M., Evrendilek, F., 2019. Pyrolytic kinetics, reaction mechanisms and products of waste tea via TG-FTIR and Py-GC/MS. Energ. Conver. Manage. 184, 436–447. https://doi.org/10.1016/j.enconman.2019.01.031.

Chen, S., Meng, A., Long, Y., Zhou, H., Li, Q., Zhang, Y., 2015b. TGA pyrolysis and gasification of combustible municipal solid waste. J. Energy Inst. 88 (3), 332–343. https://doi.org/10.1016/j.joei.2014.07.007.

Chen, D., Yin, L., Wang, H., He, P., 2014. Pyrolysis technologies for municipal solid waste: A review. Waste Manag. (Oxf.) 34 (12), 2466–2486. https://doi.org/10.1016/j.wasman.2014.08.004.

Chen, D., Yin, L., Wang, H., He, P., 2015a. Reprint of: Pyrolysis technologies for municipal solid waste: A review. Waste Manag. (Oxf.) 37, 116–136. https://doi.org/10.1016/j.wasman.2015.01.022.

Chew, K.W., Chia, S.R., Chia, W.Y., Cheah, W.Y., Munawaroh, H.S.H., Ong, W.-J., 2021. Abatement of hazardous materials and biomass waste via pyrolysis and co-pyrolysis for environmental sustainability and circular economy. Environ. Pollut. 278, 116836 https://doi.org/10.1016/j.envpol.2021.116836.

Criado, J.M., Málek, J., Ortega, A., 1989. Applicability of the master plots in kinetic analysis of non-isothermal data. Thermochim Acta 147(2), 377–385.https://doi.org/10.1016/0040-6031(89)85192-5.

Damartzis, T., Vamvuka, D., Sfakiotakis, S., Zabaniotou, A., 2011. Thermal degradation studies and kinetic modeling of cardoon (Cynara cardunculus) pyrolysis using thermogravimetric analysis (TGA). Bioresour. Technol. 102 (10), 6230–6238. https://doi.org/10.1016/j.biortech.2011.02.060.

Dharmaraj, S., Ashokkumar, V., Pandiyan, R., Halimatul Munawaroh, H.S., Chew, K.W., Chen, W.-H., Ngamcharussrivichai, C., 2021. Pyrolysis: An effective technique for degradation of COVID-19 medical wastes. Chemosphere 275, 130092. https://doi.org/10.1016/j.chemosphere.2021.130092.

Dhyani, V., Bhaskar, T., 2018. Chapter 2 - Kinetic Analysis of Biomass Pyrolysis. In: Bhaskar, T., Pandey, A., Mohan, S.V., Lee, D.-.-J. (Eds.), Waste Biorefinery. Elsevier, S.K. Khanal, pp. 39–83.

Diaz Silvarrey, L.S., Phan, A.N. 2016. Kinetic study of municipal plastic waste. *Int. J. Hydrogen Energy*, **41**(37), 16352-16364.https://doi.org/10.1016/j.ijhydene.2016.05.202.

Dubdub, I., Al-Yaari, M., 2020. Pyrolysis of Mixed Plastic Waste: I Kinetic Study. *Materials* 13 (21), 4912.

Encinar, J.M., González, J.F., 2008. Pyrolysis of synthetic polymers and plastic wastes. Kinetic study. *Fuel Process. Technol.* 89 (7), 678–686. https://doi.org/10.1016/j.fuproc.2007.12.011.

Fang, S., Yu, Z., Ma, X., Lin, Y., Chen, L., Liao, Y., 2018. Analysis of catalytic pyrolysis of municipal solid waste and paper sludge using TG-FTIR, Py-GC/MS and DAEM (distributed activation energy model). Energy 143, 517–532. https://doi.org/10.1016/j.energy.2017.11.038.

Flynn, J.H., Wall, L.A., 1966. A quick, direct method for the determination of activation energy from thermogravimetric data. J Polym Sci B 4 (5), 323–328. https://doi.org/10.1002/pol.1966.110040504.

Friedman, H.L. 1964. Kinetics of thermal degradation of char-forming plastics from thermogravimetry. Application to a phenolic plastic. *J. Polym. Sci., Part C: Polym. Lett.*, **6**(1), 183-195.https://doi.org/10.1002/polc.5070060121.

Gao, N., Humphrey Milandile, M., Tariq Sipra, A., Su, S., Miskolczi, N., Quan, C., 2022. Co-pyrolysis of municipal solid waste (MSW) and biomass with Co/sludge fly ash catalyst. Fuel 322, 124127. https://doi.org/10.1016/j.fuel.2022.124127.

Garg, S., Nayyar, A., Buradi, A., Shadangi, K.P., Sharma, P., Bora, B.J., Jain, A., Asif Shah, M., 2023. A novel investigation using thermal modeling and optimization of waste pyrolysis reactor using finite element analysis and response surface methodology. Sci. Rep. 13 (1), 10931. https://doi.org/10.1038/s41598-023-37793-8.

Gotor, F.J., Criado, J.M., Malek, J., Koga, N., 2000. Kinetic Analysis of Solid-State Reactions: The Universality of Master Plots for Analyzing Isothermal and Nonisothermal Experiments. Chem. A Eur. J. 104 (46), 10777–10782. https://doi.org/10.1021/jp0022205.

Hasan, M.M., Rasul, M.G., Khan, M.M.K., Ashwath, N., Jahirul, M.I., 2021. Energy recovery from municipal solid waste using pyrolysis technology: A review on current status and developments. Renew. Sustain. Energy Rev. 145, 111073 https://doi.org/10.1016/j.rser.2021.111073.

Ingrao, C., Faccilongo, N., Di Gioia, L., Messineo, A., 2018. Food waste recovery into energy in a circular economy perspective: A comprehensive review of aspects related to plant operation and environmental assessment. J. Clean. Prod. 184, 869–892. https://doi.org/10.1016/j.jclepro.2018.02.267.

Jung, S.-H., Cho, M.-H., Kang, B.-S., Kim, J.-S., 2010. Pyrolysis of a fraction of waste polypropylene and polyethylene for the recovery of BTX aromatics using a fluidized bed reactor. Fuel Process. Technol. 91 (3), 277–284. https://doi.org/10.1016/j.fuproc.2009.10.009.

Khan, S., Anjum, R., Raza, S.T., Ahmed Bazai, N., Ihtisham, M., 2022. Technologies for municipal solid waste management: Current status, challenges, and future perspectives. Chemosphere 288, 132403. https://doi.org/10.1016/j.chemosphere.2021.132403.

Khandelwal, H., Dhar, H., Thalla, A.K., Kumar, S., 2019. Application of life cycle assessment in municipal solid waste management: A worldwide critical review. J. Clean. Prod. 209, 630–654. https://doi.org/10.1016/j.jclepro.2018.10.233.

Kissinger, H.E., 1957. Reaction Kinetics in Differential Thermal Analysis. Anal. Chem. 29 (11), 1702–1706. https://doi.org/10.1021/ac60131a045.

Laird, D.A., Brown, R.C., Amonette, J.E., Lehmann, J., 2009. Review of the pyrolysis platform for coproducing bio-oil and biochar. Biofuels Bioprod. Biorefin. 3 (5), 547–562. https://doi.org/10.1002/bbb.169.

Li, Q., Faramarzi, A., Zhang, S., Wang, Y., Hu, X., Gholizadeh, M., 2020. Progress in catalytic pyrolysis of municipal solid waste. Energ. Conver. Manage. 226, 113525 https://doi.org/10.1016/j.enconman.2020.113525.

Liu, H., Xu, G., Li, G., 2021. Pyrolysis characteristic and kinetic analysis of sewage sludge using model-free and master plots methods. Process Saf. Environ. Prot. 149, 48–55. https://doi.org/10.1016/j.psep.2020.10.044.

Lou, F., Wang, J., Sun, C., Song, J., Wang, W., Pan, Y., Huang, Q., Yan, J., 2022. Influence of interaction on accuracy of quantification of mixed microplastics using Py-GC/MS. J. Environ. Chem. Eng. 10 (3), 108012 https://doi.org/10.1016/j.jece.2022.108012.

Luo, L., Zhang, Z., Li, C., Nishu, He, F., Zhang, X., Cai, J. 2021. Insight into master plots method for kinetic analysis of lignocellulosic biomass pyrolysis. *Energy*, **233**, 121194. https://doi.org/10.1016/j.energy.2021.121194.

Lv, G., Wu, S., 2012. Analytical pyrolysis studies of corn stalk and its three main components by TG-MS and Py-GC/MS. J. Anal. Appl. Pyrol. 97, 11–18. https://doi.org/10.1016/j.jaap.2012.04.010.

Ma, W., Rajput, G., Pan, M., Lin, F., Zhong, L., Chen, G., 2019. Pyrolysis of typical MSW components by Py-GC/MS and TG-FTIR. Fuel 251, 693–708. https://doi.org/10.1016/j.fuel.2019.04.069.

Mallick, D., Sharma, P., Bora, B.J., Baruah, D., Bhowmik, R., Barbhuiya, S.A., Balakrishnan, D., 2023. Mechanistic investigation of pyrolysis kinetics of water hyacinth for biofuel employing isoconversional method. Sustainable Energy Technol. Assess. 57, 103175 https://doi.org/10.1016/j.seta.2023.103175.

Martínez-Narro, G., Royston, N.J., Billsborough, K.L., Phan, A.N. 2023. Kinetic modelling of mixed plastic waste pyrolysis. *Chem. Thermodyn. Therm. Anal.*, **9**, 100105.https://doi.org/10.1016/j.ctta.2023.100105.

Mianowski, A., Sciazko, M., Radko, T., 2021. Vyazovkin's isoconversional method as a universal approach. Thermochim Acta 696, 178822. https://doi.org/10.1016/j.tca.2020.178822.

Mishra, R.K., Mohanty, K., 2018. Pyrolysis kinetics and thermal behavior of waste sawdust biomass using thermogravimetric analysis. Bioresour. Technol. 251, 63–74. https://doi.org/10.1016/j.biortech.2017.12.029.

Moreno, A.D., Magdalena, J.A., Oliva, J.M., Greses, S., Coll Lozano, C., Latorre-Sánchez, M., Negro, M.J., Susmozas, A., Iglesias, R., Llamas, M., Tomás-Pejó, E., González-Fernández, C., 2021. Sequential bioethanol and methane production from municipal solid waste: An integrated biorefinery strategy towards cost-effectiveness. Process Saf. Environ. Prot. 146, 424–431. https://doi.org/10.1016/j.psep.2020.09.022.

Muravyev, N.V., Pivkina, A.N., Koga, N., 2019. Critical Appraisal of Kinetic Calculation Methods Applied to Overlapping Multistep Reactions. Molecules 24 (12), 2298. https://doi.org/10.3390/molecules24122298.

Navarro, M.V., López, J.M., Veses, A., Callén, M.S., García, T., 2018. Kinetic study for the co-pyrolysis of lignocellulosic biomass and plastics using the distributed activation energy model. Energy 165, 731–742. https://doi.org/10.1016/j.energy.2018.09.133.

Negro, M.J., Manzanares, P., Ruiz, E., Castro, E., Ballesteros, M., 2017. Chapter 3 - The biorefinery concept for the industrial valorization of residues from olive oil industry. In: Galanakis, C.M. (Ed.), Olive Mill Waste. Academic, Press, pp. 57–78.

Nisar, J., Nasir, U., Ali, G., Shah, A., Farooqi, Z.H., Iqbal, M., Shah, M.R., 2021. Kinetics of pyrolysis of sugarcane bagasse: effect of catalyst on activation energy and yield of pyrolysis products. Cellul. 28 (12), 7593–7607. https://doi.org/10.1007/s10570-021-04015-1.

Noori, M., Ravari, F., Ehsani, M., 2018. Preparation of PVA nanofibers reinforced with magnetic graphene by electrospinning method and investigation of their degradation kinetics using master plot analyses on solid state. J. Therm. Anal. Calorim. 132 (1), 397–406. https://doi.org/10.1007/s10973-017-6927-7.

Nzioka, A.M., Kim, M.-G., Hwang, H.-U., Kim, Y.-J. 2019. Kinetic Study of the Thermal Decomposition Process of Municipal Solid Waste Using TGA. *Waste Biomass Valorization*, **10**(6), 1679-1691.h ttps://doi.org/10.1007/s12649-017-0183-8.

Pal, S.K., Garcés-Sánchez, G., Kranert, M., Vinu, R., 2023. Characterization and evaluation of resource recovery potential of beach plastic wastes using analytical Py-GC/MS. J. Anal. Appl. Pyrol. 172, 105996 https://doi.org/10.1016/j.jaap.2023.105996.

Perejón, A., Sánchez-Jiménez, P.E., Criado, J.M., Pérez-Maqueda, L.A., 2011. Kinetic Analysis of Complex Solid-State Reactions. A New Deconvolution Procedure. J. Phys. Chem. B 115 (8), 1780–1791. https://doi.org/10.1021/jp110895z.

Pérez-Maqueda, L.A., Criado, J.M., Sánchez-Jiménez, P.E., 2006. Combined Kinetic Analysis of Solid-State Reactions: A Powerful Tool for the Simultaneous Determination of Kinetic Parameters and the Kinetic Model without Previous Assumptions on the Reaction Mechanism. Chem. A Eur. J. 110 (45), 12456–12462. https://doi.org/10.1021/jp064792g.

Said, Z., Sharma, P., Bora, B.J., Nguyen, V.N., Bui, T.A.E., Nguyen, D.T., Dinh, X.T., Nguyen, X.P., 2023. Modeling-optimization of performance and emission characteristics of dual-fuel engine powered with pilot diesel and agricultural-food waste-derived biogas. Int. J. Hydrogen Energy 48 (18), 6761–6777. https://doi.org/10.1016/j.ijhydene.2022.07.150.

Shahbeig, H., Nosrati, M., 2020. Pyrolysis of biological wastes for bioenergy production: Thermo-kinetic studies with machine-learning method and Py-GC/MS analysis. Fuel 269, 117238. https://doi.org/10.1016/j.fuel.2020.117238.

Simão, B.L., Santana Júnior, J.A., Chagas, B.M.E., Cardoso, C.R., Ataíde, C.H., 2018. Pyrolysis of Spirulina maxima: Kinetic modeling and selectivity for aromatic hydrocarbons. Algal Res. 32, 221–232. https://doi.org/10.1016/j.algal.2018.04.007.

Sipra, A.T., Gao, N., Sarwar, H., 2018. Municipal solid waste (MSW) pyrolysis for bio-fuel production: A review of effects of MSW components and catalysts. Fuel Process. Technol. 175, 131–147. https://doi.org/10.1016/j.fuproc.2018.02.012.

Sluiter, A., Hames, B., Ruiz, R., Scarlata, C., Sluiter, J., Templeton, D., Crocker, D., 2008. Determination of structural carbohydrates and lignin in biomass. Lab. Anal. Proced. 1617 (1), 1–16.

Sophonrat, N., Sandström, L., Johansson, A.-C., Yang, W., 2017. Co-pyrolysis of Mixed Plastics and Cellulose: An Interaction Study by Py-GC×GC/MS. Energy Fuels 31 (10), 11078–11090. https://doi.org/10.1021/acs.energyfuels.7b01887.

Sørum, L., Grønli, M.G., Hustad, J.E., 2001. Pyrolysis characteristics and kinetics of municipal solid wastes. Fuel 80 (9), 1217–1227. https://doi.org/10.1016/S0016-2361(00)00218-0.

Starink, M.J., 1996. A new method for the derivation of activation energies from experiments performed at constant heating rate. Thermochim Acta 288 (1), 97–104. https://doi.org/10.1016/S0040-6031(96)03053-5.

Takeo, O., 1965. A New Method of Analyzing Thermogravimetric Data. Bull. Chem. Soc. Jpn 38 (11), 1881–1886. https://doi.org/10.1246/bcsj.38.1881.

Tang, Y., Huang, Q., Sun, K., Chi, Y., Yan, J., 2018. Co-pyrolysis characteristics and kinetic analysis of organic food waste and plastic. Bioresour. Technol. 249, 16–23. https://doi.org/10.1016/j.biortech.2017.09.210.

Tejera, J., Gascó, A., Hermosilla, D., Alonso-Gomez, V., Negro, C., Blanco, Á., 2021. UVA-LED Technology's Treatment Efficiency and Cost in a Competitive Trial Applied to the Photo-Fenton Treatment of Landfill Leachate. Processes 9 (6), 1026. https://doi.org/10.3390/pr9061026.

Vyazovkin, S., Burnham, A.K., Favergeon, L., Koga, N., Moukhina, E., Pérez-Maqueda, L.A., Sbirrazzuoli, N., 2020. ICTAC Kinetics Committee recommendations for analysis of multi-step kinetics. Thermochim Acta 689, 178597. https://doi.org/10.1016/j.tca.2020.178597.

Vyazovkin, S., Koga, N., Schick, C. 2018. Handbook of thermal analysis and calorimetry: recent advances, techniques and applications.

Vyazovkin, S., Sbirrazzuoli, N., 2006. Isoconversional Kinetic Analysis of Thermally Stimulated Processes in Polymers. Macromol. Rapid Commun. 27 (18), 1515–1532. https://doi.org/10.1002/marc.200600404.

Vyazovkin, S. 2000. Modification of the integral isoconversional method to account for variation in the activation energy. *J. Comput. Chem.*, **22**(2), 178-183.https://doi.org/10.1002/1096-987X(20010130)22:2<178::AID-JCC5>3.0.CO;2-%23.

Vyazovkin, S. 2015. *Isoconversional kinetics of thermally stimulated processes*. Springer.

Wu, S., Shen, D., Hu, J., Xiao, R., Zhang, H., 2013. TG-FTIR and Py-GC–MS analysis of a model compound of cellulose – glyceraldehyde. J. Anal. Appl. Pyrol. 101, 79–85. https://doi.org/10.1016/j.jaap.2013.02.009.

Zhang, J., Chen, T., Wu, J., Wu, J., 2015. TG-MS analysis and kinetic study for thermal decomposition of six representative components of municipal solid waste under steam atmosphere. Waste Manag. (Oxf.) 43, 152–161. https://doi.org/10.1016/j.wasman.2015.05.024.